AFF-1 fusogen can rejuvenate the regenerative potential of adult dendritic trees via self-fusion

Veronika Kravtsov[1,#], Meital Oren-Suissa[1,2,#], and Benjamin Podbilewicz[1†]

[1]Department of Biology, Technion- Israel Institute of Technology, Haifa 32000, Israel

[#]These authors contributed equally to this work

[†]Correspondence to: podbilew@technion.ac.il

Additional footnotes:

[2]Present address: Columbia University Medical Center, Department of Biochemistry & Molecular Biophysics, New York, 10032, USA

Short title: Cell fusion proteins act as neuronal anti-aging molecules in *C. elegans*

Abstract

The aging brain undergoes structural changes, affecting brain homeostasis, neuronal function and consequently cognition. Neuronal dendrites are central in the formation and maintenance of neural networks, and the extent of arborization determines the synaptic properties of the neuron. The complex architecture of dendritic arbors poses a challenge to understanding age-dependent morphological alterations, behavioral plasticity and remodeling following brain injury. Here, we use the PVD polymodal neurons of *C. elegans* as a model to study how aging affects neuronal plasticity. Using confocal live imaging of *C. elegans* PVD neurons, we demonstrate major age-related progressive morphological alterations of intricate dendritic arbors. We show that insulin/IGF-1 receptor mutations (*daf-2*) fail to inhibit the progressive morphological aging of dendrites and do not prevent the minor, but significant, decline in response to harsh touch during aging. We use the PVD neurons to study how aging animals respond to neuronal trauma. We uncovered that PVD aging is characterized by a major decline in regenerative potential of dendrites following experimental laser dendrotomy. Furthermore, the remodeling of transected dendritic trees via AFF-1-mediated self-fusion can be restored in old animals by DAF-2 insulin/IGF-1 receptor mutations, and can be differentially reestablished by ectopic expression of AFF-1 fusion protein (fusogen). Thus, AFF-1 fusogen ectopically expressed in the PVD and mutations in DAF-2/IGF-1R, differentially rejuvenate some aspects of dendritic regeneration following injury.

36 **Introduction**

37 Aging is the primary risk for neuronal diseases and general cognitive decline in humans [1],
38 yet, our understanding of the process of neuronal aging at the molecular and cell biological
39 levels is still limited. In particular, very few studies have investigated the fate of complex
40 dendritic arbors during aging, and their regenerative capacity following brain injury or
41 trauma. Signaling via the DAF-2 Insulin/IGF-1 receptor is the most prominent and
42 conserved pathway that controls aging and longevity of *C. elegans*, flies, and mammals [2]. *C.*
43 *elegans* is a powerful system to study the genetics of neuronal aging and regeneration [2-4].
44 Normally, when the DAF-2/IGF-1 receptor is activated it induces a conserved PI3K/AKT
45 kinase cascade, which in turn inhibits the DAF-16/FOXO transcription factor from entering
46 into the nucleus. Reduction of *daf-2* function doubles life span, and long-lived worms are
47 considered to stay healthy for longer [2,5]. In these animals, DAF-16/FOXO affects
48 transcription of different genes that encode heat-shock proteins, antimicrobial proteins,
49 antioxidants, and other molecules, which leads ultimately to extended lifespan [6,7]. Recently,
50 aging-associated axonal morphological alterations and decline in regenerative capacity were
51 described in *C. elegans*. *daf-2* mutations delayed these age-related morphological changes
52 and improved regeneration of aged severed axons in a *daf-16*-dependent manner [8-11].
53 Moreover, in the case of GABA motor neurons, as adult animals age there is a reduction in
54 axon growth, retraction and regrowth in response to injury. Surprisingly, the decline in
55 regeneration by regrowth is controlled by *daf-16* in a cell-autonomously fashion and
56 independently of lifespan [11].

57 The process of regeneration of injured axons in vertebrates and invertebrates often
58 involves degeneration of the distal part followed by regrowth [12-14]. However, different
59 invertebrates, including nematodes and crustaceans, use membrane fusion as an alternative
60 mechanism for repair of injured axons [15-18]. Cell fusion events were also observed in the

61 brains of mammals both spontaneously and as a result of injury such as stroke [19-21], but the
62 role of these events has remained unclear [22]. In *C. elegans*, axonal regeneration via auto-
63 fusion is mediated by the fusogen EFF-1 [15,16,18]. EFF-1 is the first *bona fide* eukaryotic
64 developmental cell-cell fusion protein. It is expressed in different cell types including
65 neurons, and mediates fusion between cells by a homotypic mechanism [23-25]. Thus, EFF-1 has
66 to be expressed in both cellular membranes for them to merge and the high-resolution crystal
67 structure of EFF-1 ectodomain suggests that EFF-1 acts by a mechanism that is distinct from
68 viral-induced fusion. EFF-1, not only has to be present in both membranes for them to fuse, it
69 also appears to interact in trans forming complexes that tether and fuse the membranes [24,26].
70 We have been studying the role of fusion proteins in the PVD neuron, a polymodal
71 nociceptor that senses harsh touch to the body, cold temperature, and posture [27-30]. The PVD
72 neuron exhibits an elaborate and invariant dendritic structure, which is composed of a
73 repetitive unit that resembles a candelabrum (or a "menorah") **(Fig 1A)** [28]. These dendritic
74 trees arise and are dynamically maintained through several intrinsic and extrinsic genetic
75 pathways [28-38].
76 The PVD develops in a stereotypic fashion from the L2 larval stage to the young adult
77 [28]. The fusion protein EFF-1 mediates dendrite retraction and auto-fusion of excess branches
78 by a novel cell-autonomous pruning mechanism [28]. Thus, this fusogen maintains the
79 structural units by trimming excess branching during normal developmental arborization [28].
80 AFF-1, a paralog of EFF-1, is a second *C. elegans* fusogen displaying a more restricted tissue
81 distribution pattern [39]; AFF-1 was not found to be involved in PVD remodeling during
82 development [40]. AFF-1 and EFF-1 fusion proteins also auto-fuse epithelial and myoepithelial
83 cells to form tubes and reshape glial cells [41-44]. Moreover, it has recently been demonstrated
84 that in vertebrates auto-fusion takes place in the development of the vascular endothelium,
85 where it leads to pruning of excess blood vessels [45] in a process that remarkably resembles

86 EFF-1-mediated PVD pruning [28]. It is unknown whether PVD structure and function is

87 affected by aging and by the activity of fusion proteins.

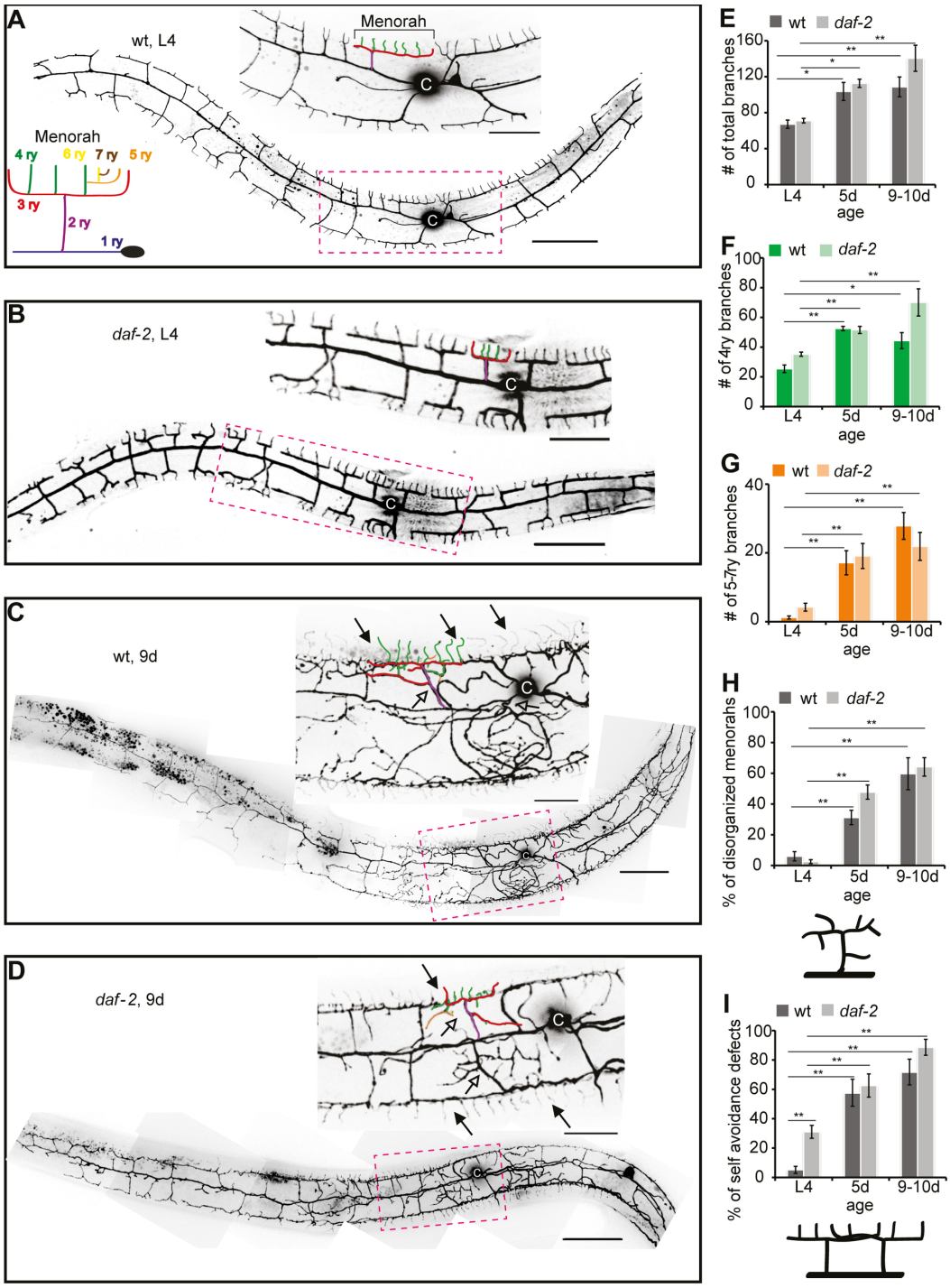

88
89

90 **Fig 1. PVD's dendritic alterations during aging**

91 **(A-D)** PVD in wild-type (wt; **A** and **C**) and *daf-2* mutants (**B** and **D**) at L4 stage and 9 days
92 of adulthood (9d). Upper panels, magnified boxed areas with candelabra-shaped units colored
93 according to the scheme (**A).** c, cell body. Scale bars, 50 µm and 20 µm in magnified images.
94 Anterior is left and ventral is down in all the figures. Filled arrows, self-avoidance defects.
95 Empty arrows, disorganized menorahs.

96 **(E-I)** Quantitation of phenotypes. Percentages were calculated for 100 µm of length around
97 the cell body. Error bars, ± s.e.m. Statistics were calculated using student's *t*-test, **P<0.01,*
98 ***P<0.001.* (**E**) There is no significant difference between wild-type animals and *daf-2*
99 mutant animals at any age (one-way ANOVA). However, there is a significant difference
100 between different developmental stages of the same genotype (*P<0.01* for wt and *P<0.0001*
101 *for daf-2).).*(**F-G**) According to ANOVA age gives a significant difference in 4ry and in 5-
102 7ry branching number both in wt and in *daf-2* backgrounds (*P<0.001* for 4ry both wt and
103 *daf-2*; 5-7ry branching *P<0.0001* for wild-type and *P<0.001* for *daf-2*).(**H-I**) According to
104 one-way ANOVA age has significance in menorahs disorganization and loss of self-
105 avoidance in both wild-type and *daf-2* (*P<0.0001* for wt and *P< P<0.0001* for *daf-2).*
106 Number of animals analyzed: *daf-2* n ≥ 8 and wild-types n ≥ 5.

107

108 Here, we show that induction of cellular fusion proteins (fusogens) can remodel and facilitate
109 regeneration of dendrites in polymodal PVD neurons of aging *Caenorhabditis elegans*. Using
110 whole-animal live imaging, we find that the PVD dendritic trees, composed of repetitive
111 orderly multibranched units, show age-dependent hyperbranching, disorganization, and loss
112 of self-avoidance. These processes, while independent of canonical lifespan-regulating
113 pathways, can be partially rescued by ectopic expression of the fusogen EFF-1 that prunes
114 multibranched dendrites. Surprisingly, most wild-type and *daf-2* (Insulin/IGF-1Receptor)
115 mutant adults that have disorganized dendritic trees have normal response to harsh touch.
116 Furthermore, we found a decreased capacity of old animals to repair laser-induced injured
117 dendrites via auto-fusion that can be restored by reducing DAF-2 function or by ectopic
118 expression of the EFF-1 paralog AFF-1 that remodels dendritic trees via merging of injured
119 branches. Our findings demonstrate that fusogens are sufficient to maintain the dendritic
120 arbor structure and increase its regeneration potential by auto-fusion in aging animals. These
121 antiaging strategies can be potentially applied to other organisms to help them recover from
122 stroke, brain trauma and spinal cord injury.

123

124

125 **Results**

126 **Progressive dendritic remodeling during aging is independent from the Insulin/IGF-1**

127 **pathway**

128 Aging neurons lose their ability to remodel following injury, change their complex

129 morphology, and may degenerate [1]. Whereas axon degeneration during aging has been

130 studied extensively both in mammals and in invertebrates, the fate of complex dendritic trees

131 in old animals has not been studied in detail in any organism. To determine how aging affects

132 the complex arborized dendritic structure, we analyzed the *C. elegans* PVD dendritic

133 branching patterns from the fourth larval stage (L4) to ten-day-old adults. We found that

134 during aging PVD's dendritic structures undergo disorganization and hyperbranching **(Figs**

135 **1A, 1C, and S1)**. Remarkably, we found that these age-dependent morphological changes of

136 the PVD dendritic pattern were not affected in long-lived animals carrying a mutation in *daf-*

137 *2* **(Figs 1A-1H, and S1)**. Adjacent PVD dendrites normally avoid each other [46], and we

138 found that as the animal ages the structural units lose their self-avoidance properties **(Fig 1C,**

139 **1D, and 1I)**. Consistently, this age-dependent dendritic pattern did not improve in *daf-2*

140 mutant animals; young *daf-2* animals at the L4 stage exhibited significantly more *daf-16*-

141 dependent self-avoidance deficiencies in comparison to wild-type **(Fig 2)**. Thus, taken

142 together our results reveal that during aging there is a *daf-2*-independent increase in

143 disorganization of branching and loss of self-avoidance.

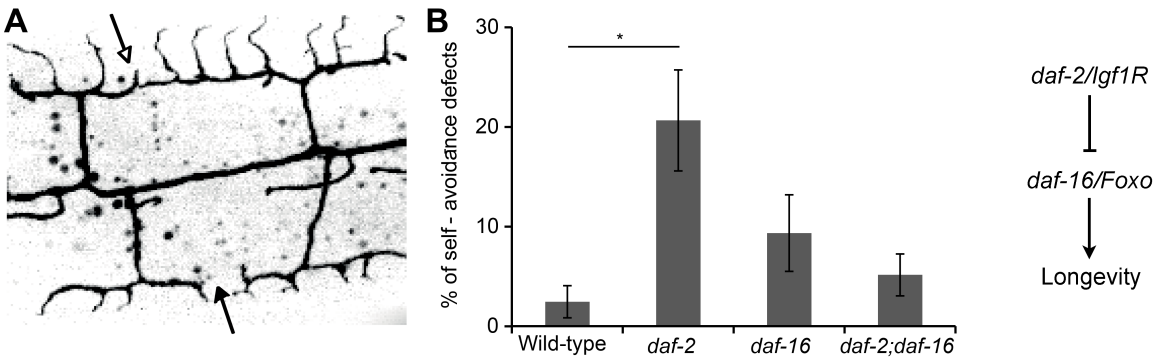

144

145 **Fig 2. DAF-2-DAF-16 control self-avoidance at L4 stage**

146 **(A)** Image showing four wild-type PVD dendritic units labeled with GFP, two of them do not
147 overlap (filled arrow) and two show defective self-avoidance (empty arrow).

148 **(B)** Percentage of defects in self-avoidance in 100 μm of length around PVD cell body at L4
149 stage in different genotypes, n ≥ 7. Defective self-avoidance increases in *daf-2* mutants in a
150 *daf-16*-dependent manner. Error bars are ± s.e.m. Statistics were calculated using ANOVA,
151 followed by *t* test, * $P<0.05$.

152 The elaborate PVD structure is highly dynamic in young animals, exhibiting constant
153 growth and retraction of individual high order branches [47-49]. To further understand the
154 dynamics of the age-dependent dendritic tree remodeling, we followed individual animals
155 over time and analyzed time-lapse movies. We found that 5-day adults still exhibited some
156 plasticity of the dendritic tree, with dynamic growth and retraction events **(Fig 3A** and **Movie**
157 **S1)**; however, both growth and retraction were two times slower **(Fig 3B)** compared to
158 younger L4 animals, imaged under the same conditions. Next we quantified the number of
159 movements of branches. Most branches showed dynamic movements ending either with
160 elongation or with shortening, but a minority of branches only grew or only retracted
161 throughout the movies. When young animals were imaged, not only the rates of growth and
162 retraction were higher, but also the number of dynamic events involving both growth and
163 retraction were higher (data not shown). Interestingly, both in L4 larvae and 5d adults there
164 were more events that ended with outgrowth or elongation rather than retraction events. We
165 also found that the decrease in dynamic events with age was proportional both for outgrowth
166 and retraction. Thus, we conclude that at all ages there are slightly more growth events than
167 retractions, which leads to branch accumulation with time and thus causing hyperbranched
168 phenotype of the PVD. These experiments reveal that the PVD dendritic arbors grow and age
169 in a dynamic way and not in a step-wise manner as apparent from still images. This dynamic
170 growth and retraction together with the increase in branching as animals age suggest that
171 hyperbranching is part of the normal dynamic growth of the dendritic arbors.

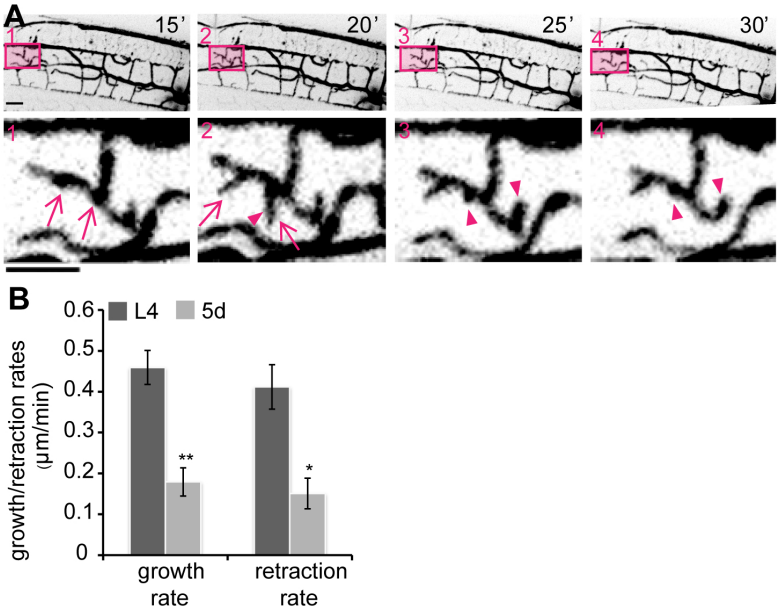

Fig 3. Adults show a reduction in dendritic plasticity

(A) Time-lapse confocal projections of 5 days of adulthood (5d) wild-type animal. Boxed areas are enlarged in the lower panel and reveal dynamic growth (arrows) and retraction (arrowheads) of branches. Scale bars, 10 µm.

(B) Growth and retraction rates in µm/minute of branches at L4 stage and 5d as measured from time-lapse movies. ≥ 18 branches were analyzed from 4 L4 animals and 2 5d animals. Error bars are ± s.e.m. *P* values from *t* tests: * *P<0.01,* ** *P<0.001*. See also **Movie S1**.

We speculated that reduced dendritic plasticity and structural changes in aged animals would affect the functionality of the PVD neurons. To shed more light on the link between structure and function of dendrites during aging, we performed a functionality test. PVD responds to harsh stimulations, and we used a classic harsh touch assay in *mec-4* mutant animals to specifically test PVD activity without the background light touch response mediated by the six light-touch mechanosensory neurons [28,50]. First, we found that although *mec-4* animals have shorter life span [10], their dendrites looked similar to wild-type between the ages L4-5d **(Fig 4)**, which further demonstrates that the morphological alterations we see are lifespan-independent. Second, we found that the PVD functionality showed a minor decrease with aging, with 5d adults presenting a small but significantly reduced harsh touch response in comparison to 1d adults, in both *mec-4* and *mec-4;daf-2* double mutants **(Fig 4F)**. We cannot rule out that multiple components of the sensorimotor circuit contribute to

192 the age-dependent decline in PVD activities. Thus, our results reveal that the morphological
193 and behavioral hallmarks of aging in PVD dendritic arbors are independent from the
194 canonical IGF-1 pathway that affects lifespan. Moreover, the fact that the dramatic increase
195 in branching and loss of self-avoidance in middle-aged animals (5d-adults; **Figs 1-3**)
196 correlates with lack of response to harsh touch in only 10% of the worms, compared to 1d
197 adults, suggests that hyperbranching, loss of self avoidance and disorganization of dendritic
198 trees might be normal and not deleterious for the behavioral response.

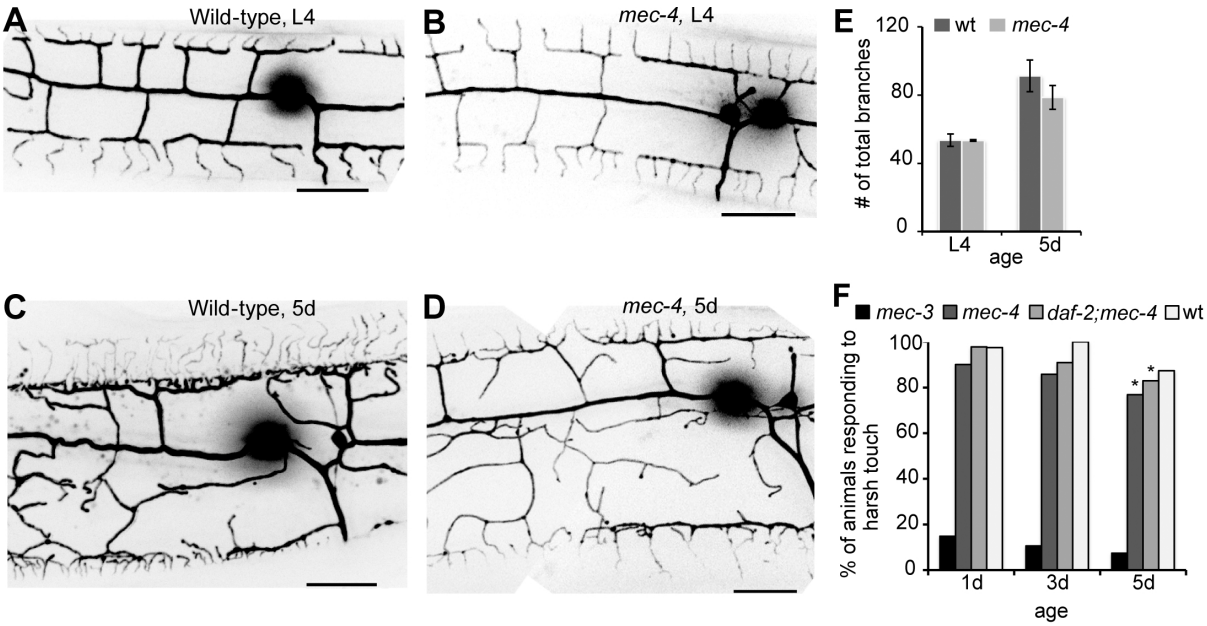

199

200 **Fig 4. Decline in response to harsh touch during aging in both wild-type and *daf-2***

201 **(A-D)** PVD's cell-body region of wt and light-touch insensitive *mec-4* mutants at the L4
202 stage and at 5 days of adulthood (5d). Scale bars are 20 µm.

203 **(E)** Total number of branches counted in 100 µm of length around cell-body in wt and *mec-4*
204 mutants at L4 and 5d (no significant differences between wt and *mec-4)*. Error bars are ±
205 s.e.m.

206 **(F)** Percentage of animals responding to harsh touch by escaping away from the stimulus. At
207 the age of 5d, the response declined in *mec-4* mutants and in *daf-2;mec-4* double mutants. *P*
208 values from $\chi 2$ test as compared between 1d to other ages (3d or 5d) for each genotype: * P
209 <0.05. Number of animals: *mec-3* ≥ 50; *mec-4* ≥ 70; *daf-2;mec-4* ≥ 40; wt ≥ 26.

210

211 In summary, the changes in dendritic architecture are not necessarily a deleterious aspect of
212 aging, but could actually be part of normal neuronal maintenance that keeps the cell
213 functioning over time. The fact that they are not altered in *daf-2* mutants supports this idea, as

214 does the functional data that shows most of the neurons function fine in 5 days adults (**Fig 4**).
215 Thus, the observed increase in dendrite branching and the disorganized appearance of the
216 trees is probably adaptive as the animals increase in girth.

217 **Age-dependent decline in dendrite regeneration is dependent on Insulin/IGF-1**

218 Mammalian axons regenerate better in younger individuals than in adults [51]. Similarly, axonal
219 regenerative ability declines drastically as nematodes advance through development and age
220 [11,52]. Our knowledge is still poor on the regenerative capacity of the dendrite, and how aging
221 affects this process of neuronal repair [53-55]. To study dendritic regeneration we severed the
222 primary dendrites of PVD neuron in aging adults. Typically, the PVDs show robust
223 regeneration at L4 larval stage, consisting in dendrite sprouting from the proximal fragment
224 still attached to the cell body and reconnection via fusion with the separated distal dendrite
225 fragment **(Fig 5A, Movie S2)**. To directly measure reconnection by auto-fusion, we used the
226 photoconvertible reporter Kaede **(Fig S2 and Movie S3)**. If fusion fails to occur, the
227 detached distal part eventually degenerates. We found that 2-3 day-old wild-type adults
228 respond more slowly to laser dendrotomy in comparison to L4 and young adults (~70% of the
229 young animals presented regeneration, whereas at the age of 2-3d neither regeneration nor
230 degeneration occurred within 3-6 hours (**Fig 5E and Movie S4)**. At the age of 5 days, the
231 ability to regenerate by dendrite auto-fusion was almost completely lost **(Fig 5C** and **5F)**.
232 Thus, we found that relatively young adults already show a decline in their dendritic
233 regenerative ability.

234 To determine whether the decline in the ability to remodel dendrites by auto-fusion is
235 dependent on the Insulin/IGF-1 pathway we tested whether the long-lived *daf-2* mutants are
236 prevented from losing their dendritic self-fusion ability. We found that *daf-2* mutants showed
237 similar regeneration to wild-type at L4 stage **(Fig 5B** and **5F)**, whereas at older age (5d) *daf-2*
238 mutants had a much higher regenerative ability than wild-types (70% successful regeneration

239 in *daf-2* versus 12.5% in wild-type) **(Fig 5D** and **5F)**. Similarly to axonal response to injury

240 [11], we found that DAF-2 inhibits regeneration of aged dendrites through inhibition of DAF-

241 16, as *daf-16* mutants and *daf-2;daf-16* double mutants showed regenerative decline during

242 aging similar to wild-type **(Fig 5F)**. In conclusion, our results reveal that dendrite

243 regeneration following transection declines with aging, a phenotype that is dependent on

244 DAF-2/IGF-1R and its target DAF-16/FOXO.

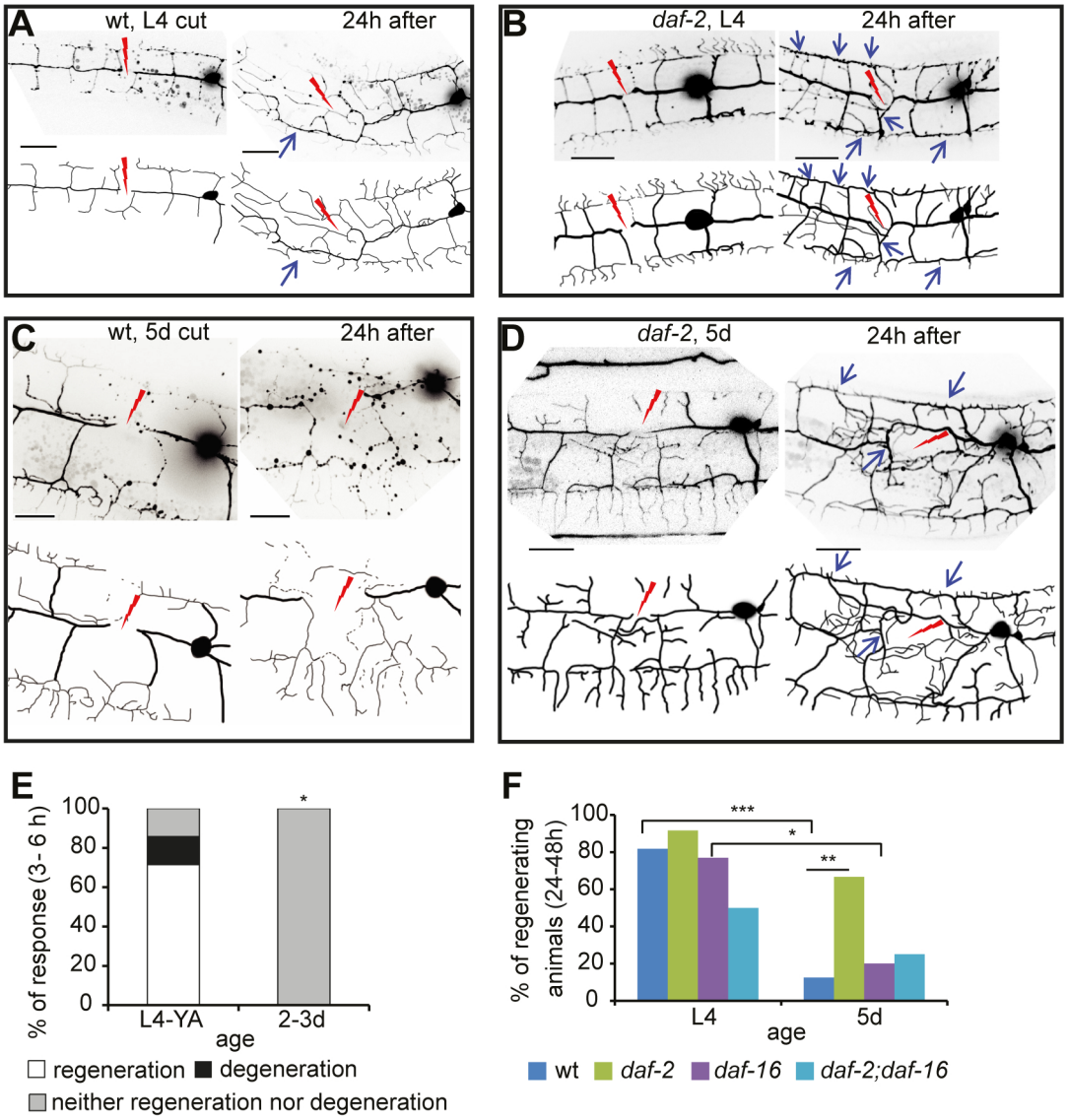

245

246

247 **Fig 5. *daf-2*(-) restores regenerative ability of aged animals via *daf-16***

248 **(A-D)** PVD neurons immediately after cut and 24 h later in wild-type and *daf-2* mutants at L4
249 and 5 days of adulthood (5d), as indicated. Schematic illustrations below negative images.
250 Red lightings, injury sites. Blue arrows, fusion sites (successful regeneration). Scale bars, 20
251 µm.

252 **(E)** Response to injury of wild-types at L4-young adult (YA) and 2-3d within a short time (3-
253 6 h) after injury. Number of animals: n=7 (L4 –YA) and n=4 (2-3d).

254 **(F)** Percentage of successfully regenerating animals within 24-48 h post injury. *p* values from
255 *Fisher's exact tests*: * $p<0.05$, ** $p<0.01$, *** $p<0.001$. Number of animals: n ≥ 8. See also
256 **Fig S3** and **Movies S2-S4**.

257

258 **AFF-1 mediates and restores dendrite regeneration in aged animals**

259 AFF-1 (Anchor cell Fusion Failure 1), is a transmembrane protein related to EFF-1 that
260 executes several cell-cell fusion events during development in the epidermis, excretory,
261 digestive and reproductive systems [39]. *aff-1* mutants have no evident morphological
262 phenotypes in the PVD neuron and its expression has not been detected in the PVD (**Fig S3**);
263 moreover, when AFF-1 is ectopically expressed in the PVD in an *eff-1* mutant background it
264 does not retract excess branching, demonstrating that it is unable to rescue the pruning
265 defects of *eff-1* **(Fig S4)**. This result shows that EFF-1 and AFF-1 fusion proteins have
266 different activities and are not interchangeable in the PVD neuron. However, AFF-1 is
267 required for dendrite fusion in response to injury in L4s and young adults [40]. Adults carrying
268 loss-of-function mutations in *aff-1* have severe egg laying defects, shorter life spans and
269 excretory system defects that prevented us from studying regeneration in aging *aff-1* mutant
270 animals. To investigate whether AFF-1 can restore the regenerative ability of dendrites in
271 older animals we overexpressed AFF-1 specifically in the PVD (PVDp::AFF-1; **Fig S5**). We
272 found that the structural units of young animals expressing PVDp::AFF-1 appeared
273 morphologically wild-type and responded similarly to dendrotomy **(Fig 6A, Movie S5)**.
274 However, when 5-day old PVDp::AFF-1 animals were dendrotomized, the percentage of
275 regenerating worms by dendrite fusion was significantly higher compared to wild-type
276 animals (60-80% and 13%, respectively; **Fig 6B and 6C, Movie S6)**. Thus, AFF-1-specific
277 overexpression in the PVD enables dendrite regeneration via auto-fusion of cut dendrites in
278 older animals **(Fig 6C)**. This autonomous and ectopic expression of the fusion protein AFF-1
279 in the PVD appears to rejuvenate the ability to reconnect cut dendrites by the self-fusion

280 mechanism. Since endogenous AFF-1 expression cannot be detected in the PVD ([40]; Fig. S3),

281 it appears that ectopic activity of the AFF-1 fusion protein in the PVD neuron is sufficient to

282 repair and remodel severed dendrites via the mechanism of auto-fusion in middle aged adults.

283

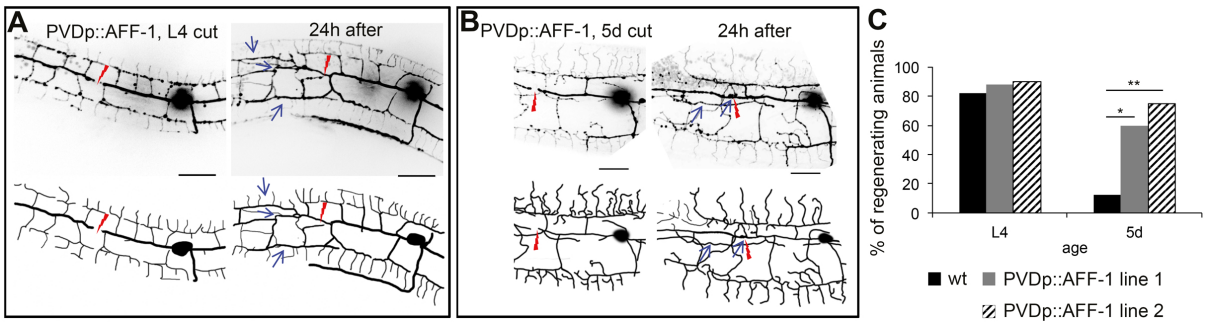

284

285

286 **Fig 6. AFF-1 enhances regeneration by dendrite fusion in 5d-old animals**

287 **(A-B)** Inverted fluorescence images of PVD neurons immediately after cut and 24 hours (h)
288 later in animals overexpressing AFF-1 in the PVD (PVDp::AFF-1), at L4 and 5 days of
289 adulthood (5d), as indicated on each image (schematic drawings below each image). Red
290 lightning marks the injury site and blue arrows point at dendrite fusion sites**.** Scale bars, 20
291 µm.

292 **(C)** Percentage of successfully regenerating animals within 24-48h after injury. *p* value from
293 *Fisher's exact test*: * $P<0.05$; ** $P<0.001$. Number of animals: $n \geq 10$. See also **Movies S5-**
294 **S6**. PVDp::AFF-1 line 1 and 2 correspond to worms carrying the extrachromosomal arrays
295 *hyEx390* and *hyEx391,* respectively.

296

297 **Rejuvenation of fusion potential of cut dendrites by *daf-2(-)* and AFF-1(+)**

298 We wished to further compare the regenerative modalities of AFF-1 overexpression and *daf-*

299 *2* mutation following dendritic laser-induced severing in aging animals. Dendritic fusion

300 following injury can occur by three possible pathways: 1) 3ry-3ry branch fusions that bypass

301 the injury site ("menorah-menorah" fusion); 2) fusion of the proximal primary (1ry) branch to

302 the detached distal 1ry; 3) both 3ry-3ry fusion and 1ry-1ry fusion **(Fig 7A)**. To determine

303 whether the mechanism of remodeling of dendritic trees following injury is distinct in wild-

304 type, *daf-2* reduced function mutants and in animals ectopically expressing AFF-1 in the

305 PVD, we compared the remodeling of dendritic trees in aging animals in these three

306 genotypes following injury. We found that in wild-type and PVDp::AFF-1 animals at the L4
307 stage, the most prevalent mechanism of repair is 3ry-3ry fusion (pathway 1), whereas in *daf-2*
308 mutants 3ry-3ry fusion together with 1ry-1ry fusion (pathway 3) increased compared to wild-
309 type **(Fig 7B-7D)**. In wild-type, we found degeneration in 50% (2-4d) and 80% (5-6d) of the
310 dendrotomized animals **(Fig 7E** and **7H)**. Adult *daf-2* mutant animals (5-6d) presented a
311 response to injury that resembled that observed in L4 wild-type animals, with 70% of the
312 animals showing regeneration, mainly via 3ry-3ry fusions **(Fig 7F** and **7I)**. In contrast, in
313 PVDp::AFF-1 animals the response to injury followed a different mechanism, with more
314 regeneration via enhanced 1ry-1ry fusion instead of 3ry-3ry fusion as observed in *daf-2*
315 mutants (Fig 7G and 7J). However, the AFF-1 effect was unrelated to longevity as
316 PVDp::AFF-1 animals had normal lifespans **(Fig S6)**. Thus, differential activities of AFF-
317 1(+) and *daf-2*(-) maintain the remodeling potential of aging arbors, and the mechanisms of
318 rejuvenation by fusion that prevent degeneration appear to be independent. In both cases
319 degeneration of the distal trees is prevented.
320 Aged dendritic trees lose their regenerative potential because following laser-induced
321 dendrotomy old neurons usually fail to auto-fuse broken dendrites and undergo degeneration.
322 DAF-2/ IGF-1R negatively regulates the regeneration process. When the fusogen AFF-1 is
323 ectopically expressed in the PVD neuron it has an anti-aging activity that promotes auto-
324 fusion of old transected primary dendrites.
325

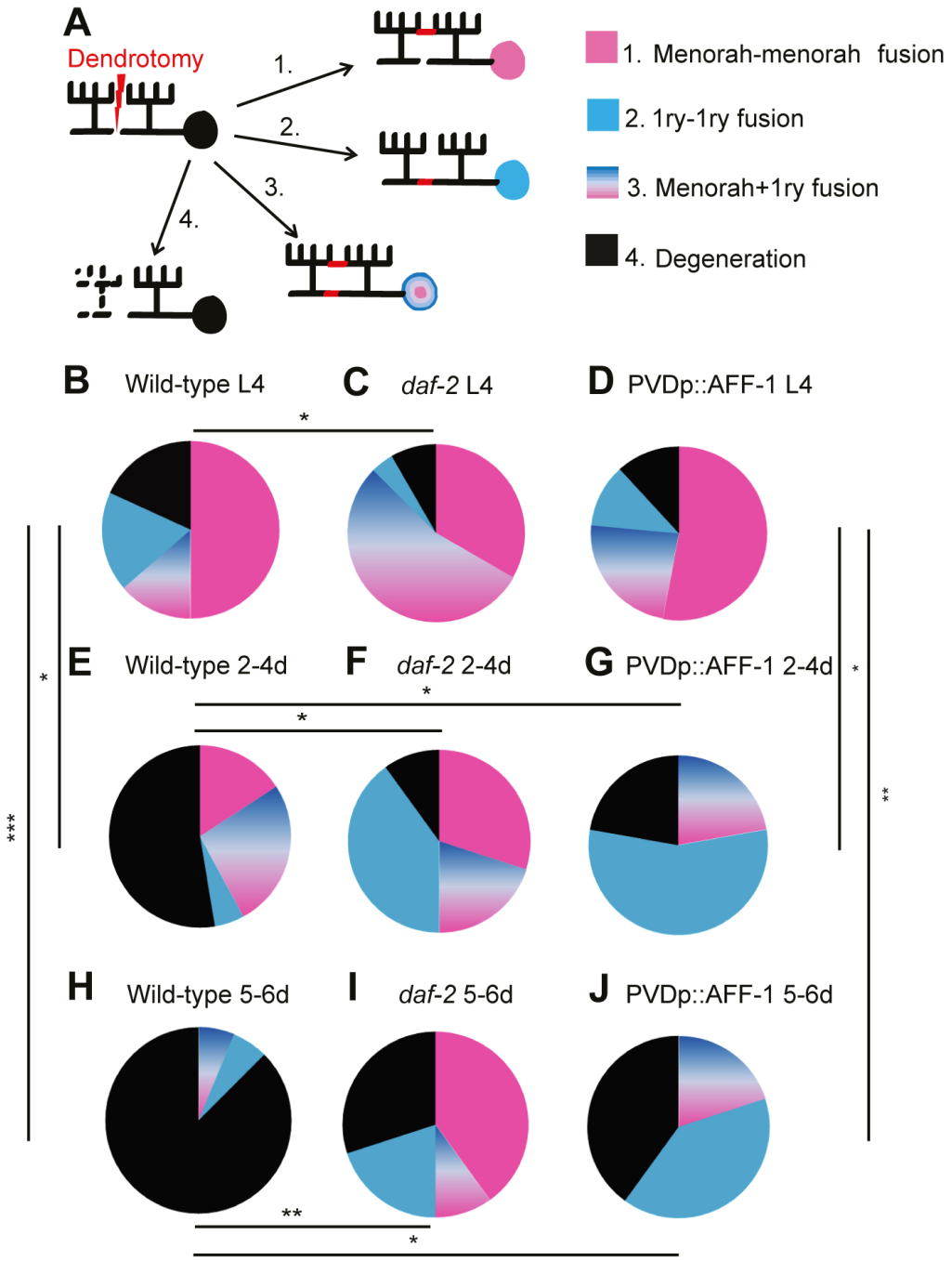

Fig 7. *daf-2*(-) and AFF-1(+) rejuvenate fusion potential of broken dendrites

(A) Cartoon representing four possible outcomes of dendrotomy. Dendrite auto-fusion indicates successful regeneration (outcomes 1-3), if fusion does not occur degeneration takes place (outcome 4).

(B-J) Percentages of wild-type worms (wt), *daf-2* mutants and AFF-1 overexpressing animals (PVDp::AFF-1) at different ages, divided into the four different types of response to injury as described in (**A**). Genotype and age are listed above each plot. *p* values from *Fisher's exact tests*: * $p<0.05$, ** $p<0.01$, *** $p<0.001$. Additional significant differences were found between: (**C** and **F**), (**C** and **I**) and between (**B** and **J**) ($p<0.05$).

339 **Discussion**

340 Precise dendritic arborization is critical for proper functioning of neuronal networks, while
341 defective dendritic development and maintenance lead to neuropathologies [56,57]. There is
342 evidence from mammalian CNS showing increase in number and length of terminal dendritic
343 arbors during aging, and reduced arborization in senile dementia [58]. However, it remains
344 unclear whether there is a direct link between altered dendritic structure and reduced function
345 in mammals. Axons of aging neurons also show altered morphologies in diverse species. In
346 *C. elegans* these axonal alterations are not affected by organismal longevity [11,51,52,59]. Here we
347 also found that dendritic alterations during aging are not affected by chronological age;
348 however, unlike the PVD dendrites, in axons the *daf-2* mutation was found to delay the
349 morphological alterations of aged animals [8-10]. Nevertheless, the *daf-2* effect in age-related
350 axonal branching was reported to be uncoupled of its role in extending the lifespan of the
351 worms [8,9]. It thus appears that DAF-2 is specifically involved in cell-autonomous pathways
352 that maintain axonal, but not dendritic morphology. We observed a small but significant
353 decline in response to harsh touch during aging in both wild-type and *daf-2* (Fig. 4). Thus,
354 we propose that the dendrite overgrowth observed in old animals reveal a reduction in
355 morphological plasticity and a normal change in the architecture of the dendritic trees that do
356 not appear to have major functional consequences in the ability to respond to noxious
357 mechanosensory stimuli. However, the link between structure and function needs to be
358 further investigated in future studies. While progressive age-related hyperbranching of the
359 PVD arbors was independent of insulin/IGF-1 pathway, overexpression of EFF-1 in the PVD
360 was sufficient to partially rescue this phenotype in old animals (**Fig S7**). EFF-1 appears to
361 act cell-autonomously to simplify the dendritic trees via its pruning activity mediated by
362 branch retraction [28].

363 We further found that dendrite regeneration following PVD dendrotomy decreases
364 with age. This decline was "rescued" in *daf-2* mutants (**Fig 5**). Axonal regeneration is
365 known to decline with age in different organisms [11,51,52,59-61]. In GABA neurons of *C. elegans*
366 the decline in axonal regeneration is also delayed in *daf-2* mutants [11]. However, these neurons
367 do not engage in self-fusion during regeneration, whereas in PVD dendrites the main
368 outcome of regeneration is auto-fusion. Recently, an important role of auto-fusion during
369 axonal regeneration was demonstrated in the PLM sensory neurons of *C. elegans*, a process
370 mediated by the fusogen EFF-1 [15,18]. In the PVD EFF-1 is not necessary for dendrite
371 reconnection following injury [40]. In the PVD dendrites, this role is fulfilled by the EFF-1
372 paralog AFF-1. Significantly, when AFF-1 is ectopically expressed, this fusogen plays a role
373 in maintenance of regenerative potential during aging (**Figs 7 and 8**). These findings
374 highlight fusion mechanisms as potential target for pharmacological intervention in
375 neuropathologies that result from both injury and aging.

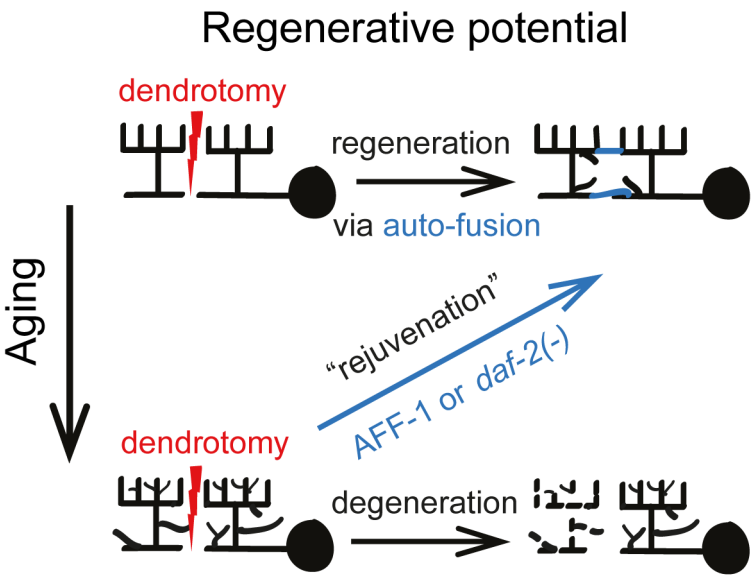

376

377 **Fig 8. Model for rejuvenation of the regenerative potential of dendritic arbors**
378 Aged multibranched neurons lose their ***regenerative potential*** because following laser-
379 induced dendrotomy old PVDs usually fail to auto-fuse broken dendrites and undergo
380 degeneration. DAF-2/ IGF-1R negatively regulates the regeneration process. When the
381 fusogen AFF-1 is ectopically expressed in the PVD neuron it has an anti-aging activity that
382 promotes auto-fusion of old transected primary dendrites.
383

384 **Materials and Methods**

385 **Nematode strains**

386 Animals were maintained at 20°C, unless otherwise stated, according to standard protocols [62].
387 All experiments were performed on hermaphrodites. N2 served as wild-type, and the
388 following mutants and transgenic strains were used:
389 NC1841 *[wdIs52(F49H12.4::GFP); rwIs1(pmec-7::RFP)]* [29], outcrossed 4X, CHB392
390 *[hmnEx133(ser-2prom3::kaede)],* kindly provided by Candice Yip and Max Heiman [63],
391 BP709 *[hmnIs133 (ser-2prom3::kaede)]*, kindly provided by Tamar Gattegno, MF190
392 *[hmIs4(des-2::gfp, pRF4)]* [28]. CB1338 *[mec-3(e1318)IV]*, *Caenorhabditis* Genetics Center
393 (CGC), CB1611 *[mec-4(e1611)X],* (CGC), BP176 *[hyEx23(des-2::eff-1, des-2::gfp, pRF4)]*
394 [28], BP177 *[hyEx392(des-2::eff-1, des-2::gfp, pRF4)],* BP488 *[eff-1(hy21)II; hmIs4;*
395 *hyEx39(des-2p::AFF-1,myo-2::GFP,KS)]*, BP906 *[daf-2(e1370)III; wdIs52; rwIs1],* BP911
396 *[hyEx39; hmnEx133]*, BP915 *[hyEx39; hmnIs133]*, BP551 *[hyEx391(des-2p::AFF-1, myo-*
397 *2::GFP, KS); hmnEx133],* BP919 *[daf-2(e1370)III; daf-16(mu86)I; hmnIs133],* BP923
398 *[daf-16(mu86)I; hmnIs133]*, BP924 *[daf-2(e1370)III; hmnIs133]*, BP925 *[mec-4(e1611)X;*
399 *hmnIs133],* BP926 *[daf-2(e1370)III;mec-4(e1611)X; hmnIs133],* BP1056 *hyEx68[AFF-*
400 *1::TY1::EGFP::3xFLAG, pRF4, KS]; dzIs53[F49H12.4p::mCherry], AFF-*
401 *1::TY1::EGFP::3xFLAG* was kindly provided by transgenome project [64], BP500 *zzIs22*
402 *[pJdC41(eff-1p::EFF-1::GFP), pRF4]; dzIs53 (pF49H12.4::mCherry) zzIs22* was kindly
403 provided by William Mohler [65].

404 **Molecular Biology**

405 The *ser-2prom3::Kaede* (pCY2 plasmid) is a kind gift from Candice Yip and Max Heiman [63].
406 It was constructed by digesting *ser-2prom3* with SbfI and AscI and Kaede with AscI and
407 NotI and then ligated together.

408 The *des-2p::AFF-1* construct (pME4 plasmid) was constructed by inserting an AFF-1
409 genomic fragment, digested from *hsp16.2::AFF-1* [39] with NheI and KpnI and cloned into
410 pME2 [28] cut with the same enzymes. *des-2p::AFF-1* was injected at a concentration of 0.1ng/ml
411 into *eff-1(hy21)* animals and three independent lines were obtained. For dendrotomy experiments,
412 two lines (*hyEx39* and *hyEx391*) were crossed into a wild-type background expressing the PVD
413 marker *ser-2p3::Kaede.*

414 **Live imaging of worms**

415 Time-lapse imaging and short imaging (one time point) of worms by Nomarski optics and
416 fluorescence microscopy was performed using a Nikon eclipse Ti inverted microscope with
417 Yokogawa CSU-X1 spinning disk or using the Zeiss Laser Scanning Microscope (LSM) 510
418 META. Animals were anesthetized using 0.1% tricaine and 0.01% tetramisole in M9
419 solution for 20-30 minutes, and then they were transferred to a 3% agar slide with an eyelash
420 attached to a toothpick. For short time imaging worms were often mounted on 3% agar slides
421 containing 5–10 mM NaN_3 instead. Image acquisition was done using Andor iQ or
422 Metamorph software, when using the spinning disk confocal (SDC), and Zen software when
423 using the LSM 510 meta microscope. Z-stacks were taken with PlanApochromat 60x oil
424 NA=1.4 objective using the SDC or 63x NA=1.4 objective using the LSM. Excitation of
425 GFP and green Kaede was done with 488 nm wavelength laser and 525 filter (6-15%, 50 ms
426 exposure time), RFP and red Kaede was excited with 561 nm wavelength laser and 607 filter
427 (15-20%, 50-100 ms exposure time). When using the sCMOS (Andor) camera z-stacks were
428 taken with ~0.23 μm z-step. With iXon EMCCD camera (Andor) z-stacks were taken with
429 ~0.5 μm z- step, gain was ~100. When the LSM 510 meta was used, z-step was ~0.8 μm.
430 Multidimensional data was reconstructed as maximum intensity projections using the FIJI
431 software (NIH Image). Images were prepared using Imaris, FIJI and Adobe Photoshop CS5.
432 Final figures were constructed using Adobe Illustrator CS5.1.

433 **Laser dendrotomies**

434 Micropoint, pulsed nitrogen laser, or the tunable Chameleon Ultra Ti-Sapphire laser system
435 (two-photon), were used to sever the primary dendrite of the PVD. The Micropoint system
436 was used on the Nikon eclipse Ti inverted microscope with Yokogawa CSU-X1 spinning
437 disk. In order to transect neurons, we used 405 beamsplitter and 365nm dye cell and either
438 IQ or Metamorph software. We used highest levels with the attenuator plate (all the way in),
439 while the software controlled attenuator was adjusted between 80-90% when using IQ, and
440 30-50% when using Metamorph. Roughly 15 pulses at 10 Hz were administered for each cut
441 in IQ and Metamorph. For all worms the primary dendrite was injured anterior to cell body.
442 Animals were imaged and a z-stack was collected immediately after cut to confirm that the
443 injury was successful.

444 The two-photon system was used on the Zeiss LSM 510 META microscope. The
445 laser produces 200fs short pulses at 113MHz repetition rate and energy of 5nJ. In order to
446 cut neurons we used 820 nm wavelength and 20-30% laser power using the Zen software.
447 Worms were imaged immediately after cut to confirm that the injury was successful, and z-
448 stacks were taken using the spinning disk confocal system or the LSM 510 META as
449 described for live imaging of worms. After surgery, animals were recovered on NGM agar
450 plates seeded with OP50 in a drop of M9 and imaged again later, or time-lapse movies were
451 immediately acquired.

452 Regeneration was defined as continuation of the fluorescent signal between the distal and
453 proximal ends or using Kaede photoconversion (**Fig S3**; see below). Significant differences
454 between ages and genotypes were determined using *Fisher's exact test.*

455 **Kaede photoconversion**

456 In order to verify that dendrites fuse as response to injury we used the photoconvertible
457 protein Kaede driven by a PVD specific promoter *ser-2prom3* [63]. Irreversible

458 photoconversion of the green Kaede to red Kaede was achieved using Mosaic system on the
459 Nikon eclipse Ti inverted microscope with Yokogawa CSU-X1 spinning disk, at 405 nm, 20-
460 50 ms exposure time with 10-20 repeats across the region of interest, which was always the
461 cell body, using either IQ or Metamorph software.

462 **Morphological quantitation of the PVD**

463 Branch count and disorganization of PVD structural units (menorahs) was counted in the 100
464 μm around cell body (unless otherwise stated), as previously described [28]. Lack of self-
465 avoidance between adjacent menorahs was determined in the same region as previously
466 described [46]. Z-stack maximum intensity projections of time-lapse movies were analyzed
467 manually, using FIJI software. Factorial analysis of variance (ANOVA) and *t-tests* were
468 performed to compare between genotypes and ages.

469 **Harsh touch assay**

470 Harsh touch assay was performed as previously described [28,50] and the experimenter was
471 blind to the genotype. The experiments were done in light touch mutant background (*mec-*
472 *4(e1611)*) [66]. *mec-3(e1338)* worms were used as negative control [50]. Significant differences
473 between the ages were determined by the $\chi 2$ test.

474 **Life-span assay**

475 Lifespan assays were carried out at 20°C as previously described [67]. A population of worms
476 was synchronized using hypochlorite and NaOH solution and ~100 animals at the L4
477 "Christmas tree" stage were placed on NGM plates containing 49.5 μM 5-Fluoro-2′-
478 deoxyuridine (FUDR, Sigma, F0503) seeded with OP50 *E. coli*, at a density of 20 worms per
479 6 cm plate. Adult day 1 was designated as the day after the L4 larval stage that served as
480 time 0. Animals were scored as dead or alive every 2-3 days until all animals died. An
481 animal was scored dead when it did not move or react at all to prodding with a platinum wire.
482 Animals that crawled off of the plate, were trapped in fungal infection, "exploded" (i.e.,

483 showed extruded tissue from the vulva), or showed internal hatching ("bagging"), were
484 excluded. If plates were contaminated, animals were transferred to fresh plates, using
485 platinum wire. Statistical significance was determined using the Log-Rank (Mantel-Cox)
486 test.

487 **RNA Isolation, Reverse Transcription, and Quantitative Real-Time PCR.**

488 Total RNA from Wild-type worms and des-2p::AFF-1 transgenic worms was isolated using
489 the RNeasy Micro kit following the manufacturer's protocol (Qiagen). RNA was used for
490 cDNA synthesis using the qScript cDNA Synthesis Kit (Quanta BioSciences) with random
491 primers. Real-time PCR was performed using AFF-1 and Fast SYBR® Green Master Mix
492 (Applied Biosystems). The PCR amplification conditions were as follows: 40 cycles of 95 °C
493 for 20 s and 60 °C for 20 s. Each PCR was run in triplicate. Data analysis and quantification
494 were performed using StepOne software V2.2 supplied by Applied Biosystems. To account
495 for the variability in the initial concentration of the RNA, results were normalized to the
496 ACT-1 housekeeping gene.

497 **Statistical analysis**

498 Statistical analysis was performed using the GraphPad online tool:
499 http://www.graphpad.com/quickcalcs/ for *t-tests, Fisher's exact test*s and χ^2 tests. Analysis of
500 variance (ANOVA) that was performed when more than two groups were compared and Log-
501 Rank survival test, using SPSS. *Freeman-Halton* extension of the *Fisher's exact test* (for 2x4
502 contingency table) was performed using the Vassarstats.net online tool, to compare between
503 the distributions of response to injury between different genotypes and ages.

504 **Acknowledgments**

505 We thank D. Cassel, M. Hilliard, and A. Sapir for critically reading earlier versions of the
506 manuscript. M. Heiman and C. Yip for providing CHB392, C. Smith and D. Miller for
507 NC1841, and T. Gattegno for BP709. We also want to thank R. Kishony and all members of

the Podbilewicz laboratory for discussion. Some strains were provided by the CGC, which is funded by NIH Office of Research Infrastructure Programs (P40 OD010440).

Author contributions: VK, MOS and BP designed the experiments. VK performed most experiments. MOS developed the system to study neuronal degeneration and regeneration following dendrotomy using the PVD neurons. MOS generated the PVDp::AFF-1 and PVDp::EFF-1 transgenics and MOS and VK tested the effects of EFF-1 and AFF-1 over-expression on regenerating animals. BP supervised this work. VK, MOS and BP wrote the paper.

The authors declare no conflict of interest.

This article contains supporting information including seven figures and six movies

References

1 Yankner, B. A., Lu, T. & Loerch, P. in *Annual Review of Pathology-Mechanisms of Disease* Vol. 3 *Annual Review of Pathology-Mechanisms of Disease* 41-66 (Annual Reviews, 2008).

2 Kenyon, C. J. The genetics of ageing. *Nature* **464**, 504-512, doi:10.1038/nature08980 (2010).

3 Hammarlund, M. & Jin, Y. Axon regeneration in C. elegans. *Current Opinion in Neurobiology* **27**, 199-207, doi:10.1016/j.conb.2014.04.001 (2014).

4 Ghosh-Roy, A. & Chisholm, A. D. Caenorhabditis elegans: A new model organism for studies of axon regeneration. *Developmental Dynamics* **239**, 1460-1464, doi:10.1002/dvdy.22253 (2010).

5 Kenyon, C., Chang, J., Gensch, E., Rudner, A. & Tabtiang, R. A C-elegans mutant the lives twice as long as wild- type *Nature* **366**, 461-464, doi:10.1038/366461a0 (1993).

6 Lin, K., Hsin, H., Libina, N. & Kenyon, C. Regulation of the Caenorhabditis elegans longevity protein DAF-16 by insulin/IGF-1 and germline signaling. *Nature Genetics* **28**, 139-145, doi:10.1038/88850 (2001).

7 Murphy, C. T. *et al.* Genes that act downstream of DAF-16 to influence the lifespan of Caenorhabditis elegans. *Nature* **424**, 277-284, doi:10.1038/nature01789 (2003).

8 Tank, E. M. H., Rodgers, K. E. & Kenyon, C. Spontaneous age-related neurite branching in Caenorhabditis elegans. *J. Neurosci.* **31**, 9279-9288, doi:10.1523/jneurosci.6606-10.2011 (2011).

9 Toth, M. L. *et al.* Neurite sprouting and synapse deterioration in the aging Caenorhabditis elegans nervous system. *J. Neurosci.* **32**, 8778-8790, doi:10.1523/jneurosci.1494-11.2012 (2012).

10 Pan, C.-L., Peng, C.-Y., Chen, C.-H. & McIntire, S. Genetic analysis of age-dependent defects of the Caenorhabditis elegans touch receptor neurons. *Proc. Natl. Acad. Sci. U.S.A.* **108**, 9274-9279, doi:10.1073/pnas.1011711108 (2011).

11 Byrne, A. B. *et al.* Insulin/IGF1 signaling inhibits age-dependent axon regeneration. *Neuron* **81**, 561-573, doi:10.1016/j.neuron.2013.11.019 (2014).

12 Park, K. K. *et al.* Promoting axon regeneration in the adult CNS by modulation of the PTEN/mTOR pathway. *Science* **322**, 963-966 (2008).

13 Taylor, A. M. *et al.* A microfluidic culture platform for CNS axonal injury, regeneration and transport. *Nat Methods* **2**, 599-605, doi:nmeth777 [pii] 10.1038/nmeth777 (2005).

14 Ruschel, J. *et al.* Axonal regeneration. Systemic administration of epothilone B promotes axon regeneration after spinal cord injury. *Science* **348**, 347-352, doi:10.1126/science.aaa2958 (2015).

15 Neumann, B. *et al.* EFF-1-mediated regenerative axonal fusion requires components of the apoptotic pathway. *Nature* **517**, 219-U259, doi:10.1038/nature14102 (2015).

16 Neumann, B., Nguyen, K. C. Q., Hall, D. H., Ben-Yakar, A. & Hilliard, M. A. Axonal Regeneration Proceeds Through Specific Axonal Fusion in Transected C. elegans Neurons. *Developmental Dynamics* **240**, 1365-1372, doi:10.1002/dvdy.22606 (2011).

17 Hoy, R. R., Bittner, G. D. & Kennedy, D. Regeneration in Crustacean motoneurons - evidence for axonal fusion *Science* **156**, 251-&, doi:10.1126/science.156.3772.251 (1967).

18 Ghosh-Roy, A., Wu, Z. L., Goncharov, A., Jin, Y. S. & Chisholm, A. D. Calcium and cyclic AMP promote axonal regeneration in Caenorhabditis elegans and require DLK-1 kinase. *J. Neurosci.* **30**, 3175-3183, doi:10.1523/jneurosci.5464-09.2010 (2010).

19 Paltsyn, A., Komissarova, S., Dubrovin, I. & Kubatiev, A. Increased cell fusion in cerebral cortex may contribute to poststroke regeneration. *Stroke research and treatment* **2013**, 869327-869327, doi:10.1155/2013/869327 (2013).

20 Alvarez-Dolado, M. *et al.* Fusion of bone-marrow-derived cells with Purkinje neurons, cardiomyocytes and hepatocytes. *Nature* **425**, 968-973, doi:http://www.nature.com/nature/journal/v425/n6961/suppinfo/nature02069_S1.html (2003).

21 Johansson, C. B. *et al.* Extensive fusion of haematopoietic cells with Purkinje neurons in response to chronic inflammation. *Nature Cell Biology* **10**, 575-583, doi:10.1038/ncb1720 (2008).

22 Giordano-Santini, R., Linton, C. & Hilliard, M. A. Cell-cell fusion in the nervous system: Alternative mechanisms of development, injury, and repair. *Seminars in cell & developmental biology*, doi:10.1016/j.semcdb.2016.06.019 (2016).

23 Mohler, W. A. *et al.* The type I membrane protein EFF-1 is essential for developmental cell fusion in *C. elegans*. *Dev Cell* **2**, 355-362 (2002).

24 Podbilewicz, B. *et al.* The C. elegans developmental fusogen EFF-1 mediates homotypic fusion in heterologous cells and in vivo. *Dev Cell* **11**, 471-481 (2006).

25 Shemer, G. *et al.* EFF-1 is sufficient to initiate and execute tissue-specific cell fusion in *C. elegans*. *Curr Biol* **14**, 1587-1591 (2004).

26 Pérez-Vargas, J. *et al.* Structural basis of eukaryotic cell-cell fusion. *Cell* **157**, 407-419 (2014).

27 Tsalik, E. L. *et al.* LIM homeobox gene-dependent expression of biogenic amine receptors in restricted regions of the C-elegans nervous system. *Developmental Biology* **263**, 81-102, doi:10.1016/s0012-1606(03)00447-0 (2003).

28 Oren-Suissa, M., Hall, D. H., Treinin, M., Shemer, G. & Podbilewicz, B. The fusogen EFF-1 controls sculpting of mechanosensory dendrites. *Science* **328**, 1285-1288, doi:10.1126/science.1189095 (2010).

29 Smith, C. J. *et al.* Time-lapse imaging and cell-specific expression profiling reveal dynamic branching and molecular determinants of a multi-dendritic nociceptor in C. elegans. *Dev. Biol.* **345**, 18-33, doi:10.1016/j.ydbio.2010.05.502 (2010).

30 Chatzigeorgiou, M. *et al.* Specific roles for DEG/ENaC and TRP channels in touch and thermosensation in C. elegans nociceptors. *Nat. Neurosci.* **13**, 861-U106, doi:10.1038/nn.2581 (2010).

31 Salzberg, Y. *et al.* Skin-derived cues control arborization of sensory dendrites in Caenorhabditis elegans. *Cell* **155**, 308-320, doi:10.1016/j.cell.2013.08.058 (2013).

32 Dong, X., Liu, O. W., Howell, A. S. & Shen, K. An extracellular adhesion molecule complex patterns dendritic branching and morphogenesis. *Cell* **155**, 296-307, doi:10.1016/j.cell.2013.08.059 (2013).

33 Dong, X., Shen, K. & Bülow, H. E. Intrinsic and Extrinsic Mechanisms of Dendritic Morphogenesis. *Annual Review of Physiology* **77**, null, doi:doi:10.1146/annurev-physiol-021014-071746 (2015).

34 Liu, O. W. & Shen, K. The transmembrane LRR protein DMA-1 promotes dendrite branching and growth in C. elegans. *Nat. Neurosci.* **15**, 57-U74, doi:10.1038/nn.2978 (2012).

35 Maniar, T. A. *et al.* UNC-33 (CRMP) and ankyrin organize microtubules and localize kinesin to polarize axon-dendrite sorting. *Nat. Neurosci.* **15**, 48-U66, doi:10.1038/nn.2970 (2012).

36 Cohen, E. *et al.* Caenorhabditis elegans nicotinic acetylcholine receptors are required for nociception. *Molecular and Cellular Neuroscience* **59**, 85-96, doi:10.1016/j.mcn.2014.02.001 (2014).

37 Husson, S. J. *et al.* Optogenetic Analysis of a Nociceptor Neuron and Network Reveals Ion Channels Acting Downstream of Primary Sensors. *Current Biology* **22**, 743-752, doi:10.1016/j.cub.2012.02.066 (2012).

38 Wei, X. *et al.* The unfolded protein response is required for dendrite morphogenesis. *eLife* **4**, e06963, doi:10.7554/eLife.06963 (2015).

39 Sapir, A. *et al.* AFF-1, a FOS-1-regulated fusogen, mediates fusion of the anchor cell in C-elegans. *Dev. Cell* **12**, 683-698, doi:10.1016/j.devcel.2007.03.003 (2007).

40 Oren-Suissa, M., Gattegno, T., Kravtsov, V. & Podbilewicz, B. Extrinsic repair of injured dendrites as a paradigm for regeneration by fusion. *Preprint. Available: BioRxiv*, doi:http://dx.doi.org/10.1101/062372 (2016).

41 Procko, C., Lu, Y. & Shaham, S. Glia delimit shape changes of sensory neuron receptive endings in C. elegans. *Development* **138**, 1371-1381, doi:10.1242/dev.058305 (2011).
42 Stone, C. E., Hall, D. H. & Sundaram, M. V. Lipocalin signaling controls unicellular tube development in the Caenorhabditis elegans excretory system. *Dev Biol* **329**, 201-211, doi:10.1016/j.ydbio.2009.02.030 (2009).
43 Rasmussen, J. P., English, K., Tenlen, J. R. & Priess, J. R. Notch signaling and morphogenesis of single-cell tubes in the C. elegans digestive tract. *Dev Cell* **14**, 559-569 (2008).
44 Soulavie, F. & Sundaram, M. V. Auto-fusion and the shaping of neurons and tubes. *Seminars in cell & developmental biology*, doi:10.1016/j.semcdb.2016.07.018 (2016).
45 Lenard, A. *et al.* Endothelial cell self-fusion during vascular pruning. *PLoS biology* **13**, e1002126-e1002126, doi:10.1371/journal.pbio.1002126 (2015).
46 Smith, C. J., Watson, J. D., VanHovene, M. K., Colon-Ramos, D. A. & Miller, D. M., III. Netrin (UNC-6) mediates dendritic self-avoidance. *Nat. Neurosci.* **15**, 731-737, doi:10.1038/nn.3065 (2012).
47 Oren-Suissa, M., Hall, D., Treinin, M., Shemer, G. & Podbilewicz, B. The Fusogen EFF-1 Controls Sculpting of Mechanosensory Dendrites. *Science* **328**, 1285-1288, doi:10.1126/science.1189095 (2010).
48 Smith, C. J., Watson, J. D., VanHoven, M. K., Colon-Ramos, D. A. & Miller, D. M., 3rd. Netrin (UNC-6) mediates dendritic self-avoidance. *Nat Neurosci* **15**, 731-737, doi:10.1038/nn.3065 (2012).
49 Smith, C. J. *et al.* Time-lapse imaging and cell-specific expression profiling reveal dynamic branching and molecular determinants of a multi-dendritic nociceptor in C. elegans. *Dev Biol* **345**, 18-33, doi:S0012-1606(10)00805-5 [pii] 10.1016/j.ydbio.2010.05.502 (2010).
50 Way, J. C. & Chalfie, M. The mec-3 gene of Caenorhabditis-elegans requires its own product for maintained expression and is expressed in 3 neuronal cell-types *Genes Dev.* **3**, 1823-1833, doi:10.1101/gad.3.12a.1823 (1989).
51 Verdu, E., Ceballos, D., Vilches, J. J. & Navarro, X. Influence of aging on peripheral nerve function and regeneration. *J. Periph. Nerv. Syst.* **5**, 191-208, doi:10.1046/j.1529-8027.2000.00026.x (2000).
52 Zou, Y. *et al.* Developmental decline in neuronal regeneration by the progressive change of two intrinsic timers. *Science* **340**, 372-376, doi:10.1126/science.1231321 (2013).
53 Bekkers, J. M. & Hausser, M. Targeted dendrotomy reveals active and passive contributions of the dendritic tree to synaptic integration and neuronal output. *Proc Natl Acad Sci U S A* **104**, 11447-11452, doi:0701586104 [pii] 10.1073/pnas.0701586104 (2007).
54 Rao, K. *et al.* Spastin, atlastin, and ER relocalization are involved in axon but not dendrite regeneration. *Mol Biol Cell* **27**, 3245-3256, doi:10.1091/mbc.E16-05-0287 (2016).
55 Nawabi, H., Zukor, K. & He, Z. No simpler than mammals: axon and dendrite regeneration in Drosophila. *Genes Dev* **26**, 1509-1514, doi:10.1101/gad.198150.112 (2012).
56 Jan, Y. N. & Jan, L. Y. Branching out: mechanisms of dendritic arborization. *Nat. Rev. Neurosci.* **11**, 316-328, doi:10.1038/nrn2836 (2010).
57 Koleske, A. J. Molecular mechanisms of dendrite stability. *Nat. Rev. Neurosci.* **14**, 536-550, doi:10.1038/nrn3486 (2013).
58 Buell, S. J. & Coleman, P. D. Dendritic growth in the aged human-brain and failure of growth in senile dementia *Science* **206**, 854-856, doi:10.1126/science.493989 (1979).
59 Hammarlund, M., Nix, P., Hauth, L., Jorgensen, E. M. & Bastiani, M. Axon regeneration requires a conserved MAP kinase pathway. *Science* **323**, 802-806, doi:10.1126/science.1165527 (2009).
60 Gabel, C. V., Antonie, F., Chuang, C.-F., Samuel, A. D. T. & Chang, C. Distinct cellular and molecular mechanisms mediate initial axon development and adult-stage axon regeneration in C. elegans. *Development* **135**, 1129-1136, doi:10.1242/dev.013995 (2008).
61 Pestronk, A., Drachman, D. B. & Griffin, J. W. Effects of aging on nerve sprouting and regeneration *Exp. Neurol.* **70**, 65-82, doi:10.1016/0014-4886(80)90006-0 (1980).
62 Brenner, S. Genetics of Caenorhabditis-elegans *Genetics* **77**, 71-94 (1974).
63 Yip, Z. C. & Heiman, M. G. Duplication of a Single Neuron in C. elegans Reveals a Pathway for Dendrite Tiling by Mutual Repulsion. *Cell reports*, doi:10.1016/j.celrep.2016.05.003 (2016).
64 Sarov, M. *et al.* A recombineering pipeline for functional genomics applied to Caenorhabditis elegans. *Nat Methods* **3**, 839-844, doi:10.1038/nmeth933 (2006).
65 del Campo, J. J. *et al.* Fusogenic activity of EFF-1 is regulated via dynamic localization in fusing somatic cells of C. elegans. *Curr Biol* **15**, 413-423 (2005).
66 Chalfie, M. & Sulston, J. Developmental genetics of the mechanosensory neurons of Caenorhabditis-elegans *Dev. Biol.* **82**, 358-370, doi:10.1016/0012-1606(81)90459-0 (1981).
67 Apfeld, J. & Kenyon, C. Cell nonautonomy of C-elegans daf-2 function in the regulation of diapause and life span. *Cell* **95**, 199-210, doi:10.1016/s0092-8674(00)81751-1 (1998).